Using Imaging Spectroscopy to Map Acidic Mine Waste

Gregg A. Swayze*^, Kathleen S. Smith^,
Roger N. Clark ^, Stephen J. Sutley^,
Ronald M. Pearson[†], J. Sam Vance[a],
Philip L. Hageman^, Paul H. Briggs^,
Allen L. Meier^, Michael J. Singleton[Ê]
and Shelly Roth[§]

^U.S. Geological Survey, MS 973 Box 25046
Denver Federal Center, Denver, CO 80225
†U.S. Bureau of Reclamation, P.O. Box 25007 D-
8321, Denver Federal Center, Denver, CO 80225
aU.S. Environmental Protection Agency, Region VIII
999 18th St., Suite 500, EPR-SR Unit A
Denver, CO 80202
ÊDepartment of Earth and Planetary Sciences
Campus Box 1169, Washington University
St. Louis, MO 63130
§Department of Geology and Geophysics
University of New Orleans,Lakefront
New Orleans, LA 70148
* Corresponding author phone (303) 236-0925; Fax
(303) 236-3200;email:
gswayze@speclab.cr.usgs.gov

Abstract

The process of pyrite oxidation at the surface of mine waste may produce acidic water that is gradually neutralized as it drains away from the waste, depositing different Fe-bearing secondary minerals in roughly concentric zones that emanate from mine-waste piles. These Fe-bearing minerals are indicators of the geochemical conditions under which they form. Airborne and orbital imaging spectrometers can be used to map these mineral zones because each of these Fe-bearing secondary minerals is spectrally unique. In this way, imaging spectroscopy can be used to rapidly screen entire mining districts for potential sources of surface acid drainage, and to detect acid producing minerals in mine waste or unmined rock outcrops. Spectral data from the AVIRIS instrument were used to evaluate mine waste at the California Gulch Superfund Site near Leadville, Colorado. Laboratory leach tests of surface samples show that leachate pH is most acidic and metals most mobile in samples from the inner jarosite zone and that leachate pH is near-neutral and metals least mobile in samples from the outer goethite zone.

Introduction

Acid rock drainage can adversely impact the quality of drinking water and the health of riparian ecosystems. The task of identifying sources of acid rock drainage is often costly and time consuming. With more than 48,000 inactive metal-mine sites to evaluate for potential acidic drainage in the contiguous United States (1), a rapid screening method is needed to identify those sites in need of closer inspection. Recent advancements in airborne sensors have allowed the development of such a screening tool. Airborne imaging spectrometers, such as NASA's Airborne Visible/Infrared Imaging Spectrometer (AVIRIS), are now capable of measuring reflected light in hundreds of continuous channels and producing high-quality spectra (2). Such high-spectral-resolution data contain the spectral signatures of molecular absorptions, which can be diagnostic of specific minerals, thus providing a way to map their surface distributions (3 - 4).

Acidic water formed by sulfide oxidation can precipitate a large suite of relatively soluble and insoluble Fe-bearing secondary minerals whose speciation is controlled by pH, degree of oxidation, moisture content, and solution composition (5 - 7). Minerals such as copiapite $[Fe^{II}Fe_4^{III}(SO_4)_6$-$(OH)_2 C20H_2O]$, jarosite $[(K, H_3O, Na)Fe_3(SO_4)_2(OH)_6]$, schwertmannite $[Fe_8O_8(OH)_6SO_4]$, ferrihydrite $[\sim Fe_5HO_8 C4H_2O]$, goethite $["-FeO(OH)]$, and hematite $["-Fe_2O_3]$ (8- 10) are of special interest to this study. These secondary minerals are Fe-rich and many of them are hydroxyl- and/or water-bearing, making it possible to spectrally identify them on the basis of their diagnostic spectral reflectance signatures (11). Because jarosite forms under more acidic conditions then do schwertmannite, ferrihydrite, and goethite (6), the relative distributions of these minerals can provide a remote sensing basis for locating potential acid producing areas (12).

Imaging spectrometers have been used to map minerals in hydrothermally altered areas for mineral exploration since these instruments became operational in the mid-1980's (2). Kruse and others (13) were the

first to collect imaging spectrometer data over a mining district for the sole purpose of mine waste remediation. Their efforts at Leadville, Colorado were hampered by the poor quality of the spectral data of the late 1980's. Later, King and others (*14*) used imaging spectroscopy to map the extent of acidic drainage emanating from the Summitville mine site in southwestern Colorado, a Superfund Site administered by the U.S. Environmental Protection Agency (EPA). They were able to show that the Alamosa River received contributions of metal-rich material from natural sources in addition to those from Summitville.

More recently, Farrand and Harsanyi (*15*) used imaging spectroscopy to map ferruginous sediments contaminated by mine waste along the Coeur d'Alene River in Idaho. A similar study by Fenstermaker and Miller (*16*) located mill tailings along Sixmile Canyon near Virginia City, Nevada.

The Leadville mining district, located at an altitude of 3000 m on the western slope of the Mosquito Range in the Central Colorado Rocky Mountains, has been mined for Au, Ag, Pb, and Zn since 1859 (*17*). Waste rock and tailings, rich in

Figure 1. Reflectance spectra of Fe-bearing secondary minerals and pyrite showing intense Fe-absorptions from 0.35 – 1.35 μm. Spectra offset vertically for clarity (main tick marks are 50% reflectance units apart). Spectra are from the USGS Digital Spectral Library (19) and this study.

pyrite and other sulfides, are now dispersed over a 30 km^2 area including part of the city of Leadville.

Oxidation of sulfides in these wastes releases trace metals into snowmelt and thunderstorm runoff (*18*), which drains into the Arkansas River, a main source of water for urban centers and agricultural communities in Colorado and several other states. Most of the Leadville mining district has been designated as the California Gulch Superfund Site by the EPA.
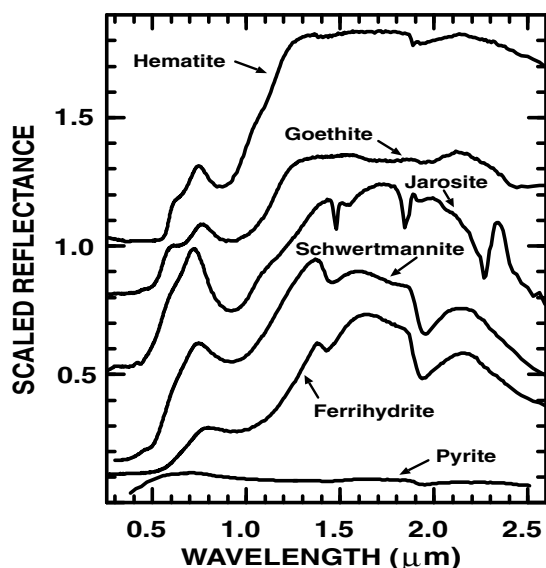
The objectives of this study were (i) to develop a rapid spectral screening tool that could map Fe-bearing mineral indicators of acidic mine waste, (ii) to investigate the connection between spectrally detectable minerals, surface pH, and metal leachability, (iii) to create a mineral map of the California Gulch Superfund Site that highlighted areas of potential acidic drainage to help guide the mine waste evaluation process, and (iv) to test how well spectral mineral maps predict acid generation and metal leachability at a specific waste pile. A leach study was undertaken to investigate whether secondary mineral zones correlated with leachate pH and metal leachability.

Methods
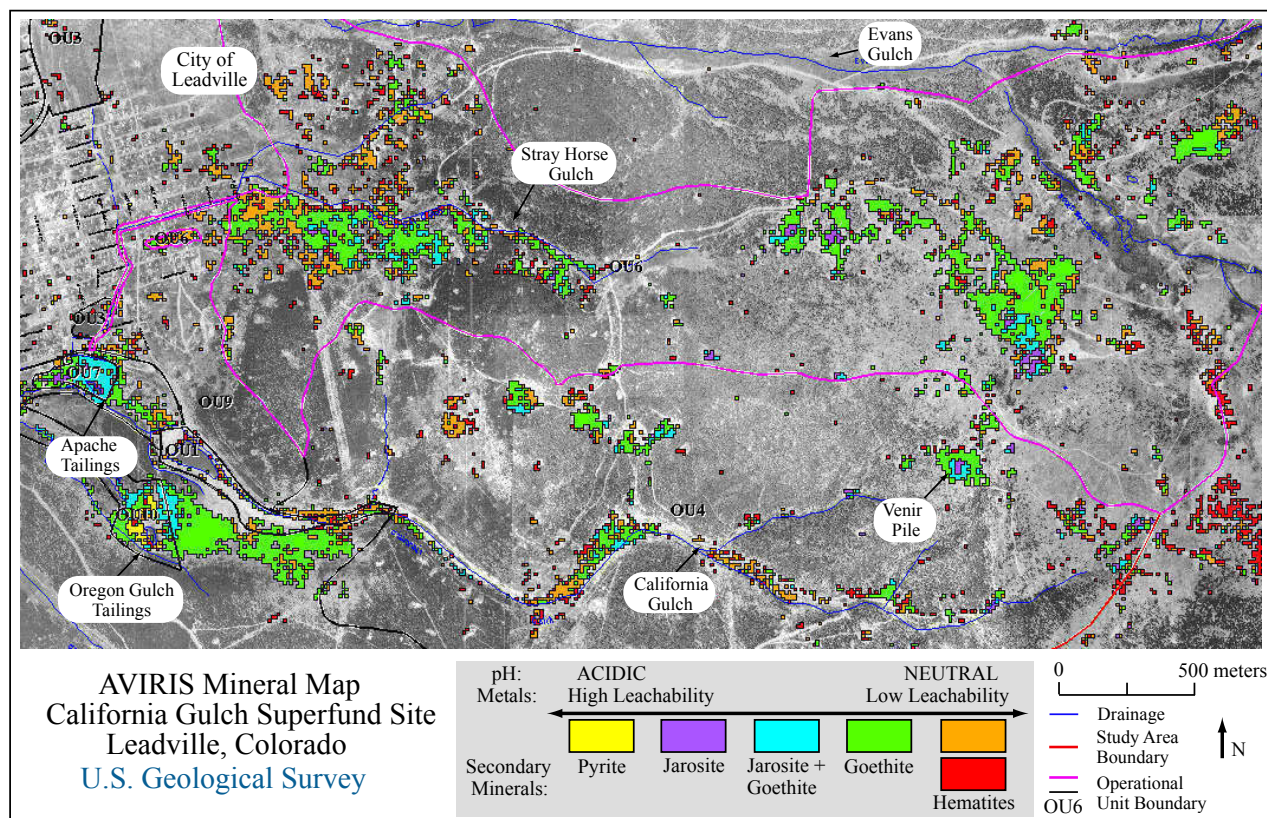
Spectrally Mapping Mine Waste with AVIRIS. Direct spectral detection of pyrite using imaging spectroscopy would be an ideal method of locating acidic mine waste at Leadville. However, pyrite's low reflectance (Figure 1), saturated Fe-absorptions, and typical coating by secondary minerals hampers its direct spectral detection. Consequently, Fe-bearing secondary minerals are much better spectral targets than pyrite. Each secondary mineral has a unique spectral signature formed by a set of distinctly shaped absorptions at slightly different wavelength positions (*19*) making it possible to spectrally distinguish each mineral (Figure 1). In this study we use the Fe-bearing secondary minerals as indicators to map acidic mine waste.

Imaging spectrometer data were collected at Leadville on July 27, 1995 by AVIRIS. This instrument, built for NASA by the Jet Propulsion Laboratory (JPL), is an airborne whiskbroom scanner that measures the reflected solar spectrum over a wavelength range from 0.4 - 2.5 μm in 224 contiguous spectral channels at 0.01 μm intervals across the spectrum (*2*). A complete spectrum is measured for each 20 x 15 m pixel on the ground producing an image 614 pixels wide (9 km wide at the altitude of Leadville) and up to 800 km in length. After routine processing at JPL, these data were calibrated at the

Figure 2. AVIRIS mineral map of Fe-bearing minerals produced using the Tetracorder algorithm, overlaid on geographically registered orthophotographic images of the Leadville mining district. AVIRIS pixels originally oriented northeast-southwest were resampled to an east-west alignment using the nearest neighbor resampling technique during the registration process, which causes minor changes in the outlines of the mineral zones.

U.S. Geological Survey (USGS) from radiance to apparent reflectance using the ATREM program (*20*) and a ground calibration site with the method described by Clark and others (*21*). Because AVIRIS measures reflected sunlight it cannot detect minerals deeper than can be seen with the human eye at visible wavelengths and only slightly deeper at near-infrared wavelengths.

Calibrated AVIRIS reflectance data were spectroscopically mapped using the Tetracorder algorithm (*3, 22*), an expert system capable of simultaneously analyzing spectra of solids, liquids, and gases. Tetracorder's primary subroutine is a modified least-squares shape-matching algorithm that compares spectra of unknown materials with hundreds of reference-library spectra and identifies the best match. The spectral library used to map Leadville AVIRIS data contained 160 reference spectra of individual pure minerals and mineral mixtures. Tetracorder utilized spectral features in two spectral regions: the electronic region (0.4 - 1.35 µm) where absorptions are caused by

transition metals (e.g., Fe, Mn, Ti, Cu, Co, and Cr) and the vibrational region (1.35 - 2.5 µm) where absorptions are caused by OH^-, H_2O, NH_4^+, SO_4^{2-}, and CO_3^{2-}. Even though a variety of minerals may have been present in the subsurface, Tetracorder mapped only those that were spectrally dominant at the optical surface, which consists of approximately the upper 50 µm of the ground surface (*23*). The spectrally dominant minerals in each spectral region were chosen for each 15 x 20 m pixel. The accuracy of Tetracorder identifications has been tested by numerical modeling and comparison of its spectral identification results with X-ray diffraction (XRD) analysis of field samples (*24*). XRD analyses of mine-waste samples, described below, provides additional checks on the performance of Tetracorder at Leadville. Other spectral mapping algorithms may be able to produce mineral maps similar to those of Tetracorder.

Color-coded mineral maps of the Leadville AVIRIS scenes were computed using the Tetracorder algorithm. To facilitate comparison with features on
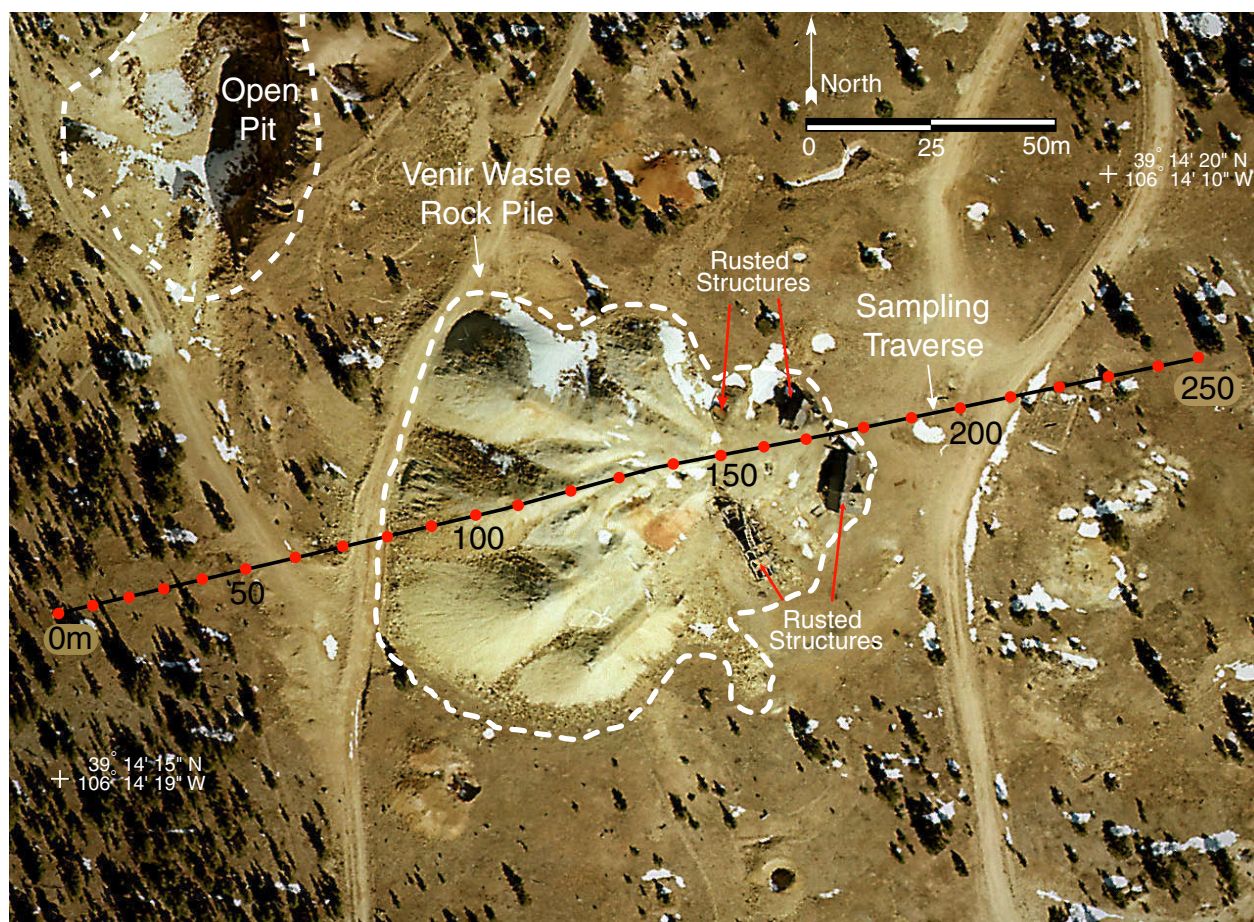
Figure 3. Venir mine-waste pile traverse collection stations (red dots) with distances in meters shown on a geographically registered color aerial photograph. White areas are snow, rectangular objects are rusted man-made structures, and dark green objects are lodgepole pines casting shadows.

the ground, the electronic-region mineral map was geographically registered and overlaid on orthophotographic images of the Leadville area (Figure 2).

Venir Pile Traverse. We chose the Venir waste rock pile, located 4 km east-southeast of Leadville at an elevation of 3,600 m, for the leach study because it has the clearest pattern of concentric secondary Fe-bearing mineral zones (Figure 2). Approximately one year after the AVIRIS overflight, 26 surficial samples from the top few centimeters of the mine waste were collected every 10 m along a 250 m traverse across the Venir pile (Figure 3). The distance interval between adjacent samples was selected to be smaller than the narrowest dimension of an AVIRIS pixel to provide a traverse sampled at a finer spatial scale than that of the AVIRIS pixel spacing. The traverse was made long enough to extend across all three spectral zones and

out into the forest on either side of the Venir waste pile.

As a check on the accuracy of the AVIRIS mineral map of the Venir pile, field spectra of each sample collection station were acquired. To achieve a signal-to-noise ratio greater than that of the AVIRIS data, 10 to 20 reflectance spectra were measured at each sample station with an Analytical Spectral Devices Full Range Spectrometer over the 0.4 - 2.5 μm range and then averaged (any use of trade, product, or firm names in this publication is for descriptive purposes only and does not imply endorsement by the U.S. Government). Spectral measurements were made continuously while traversing a 10 x 5 m ellipse of the undisturbed ground surface centered on each sample station, with the long axis of the ellipse parallel to the traverse direction. The ~35 cm diameter footprint of the instrument was effectively spread randomly over a large area within
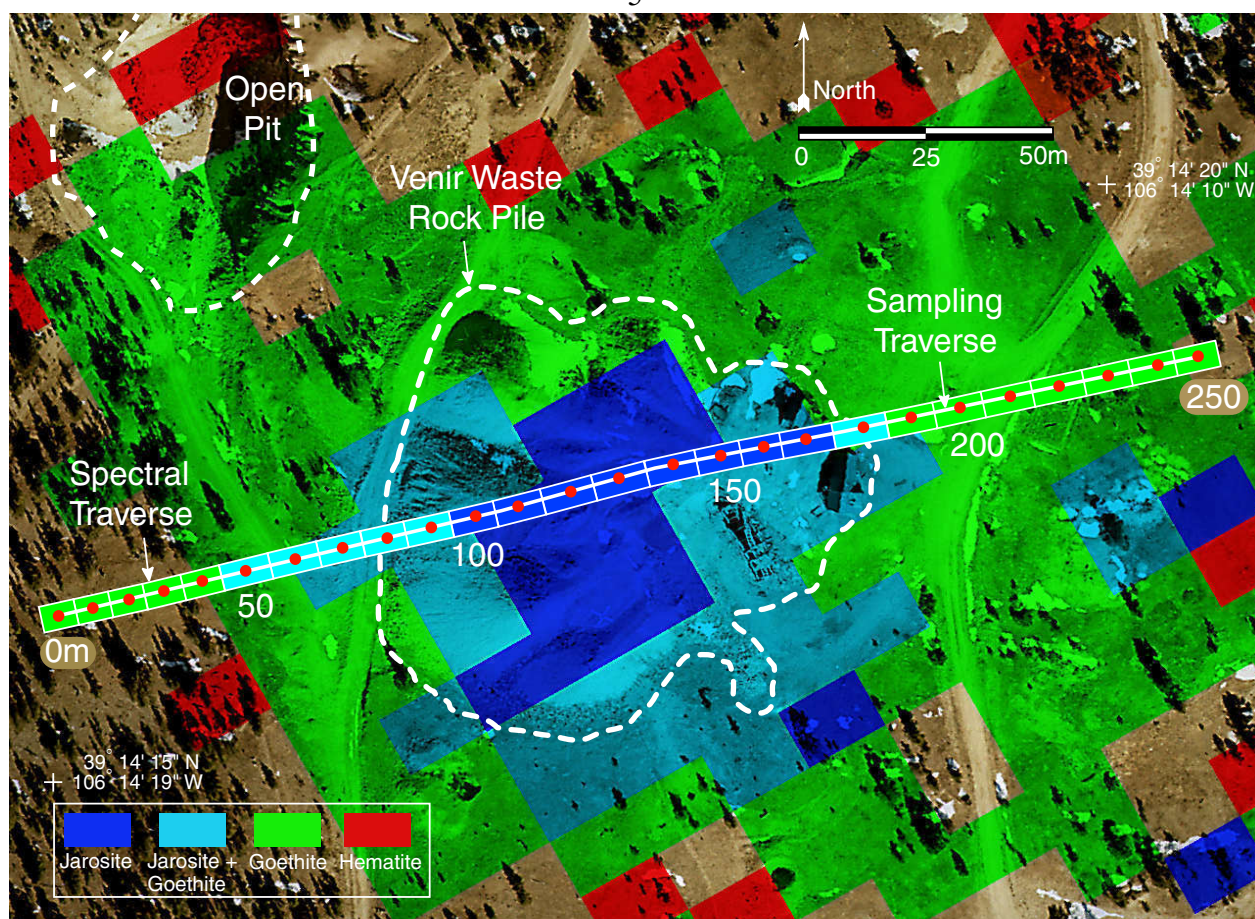
Figure 4. Spectral traverse and AVIRIS mineral maps overlaid on a high-spatial-resolution aerial photograph of the Venir mine-waste pile. Mineral maps show the spectrally dominant Fe-bearing secondary minerals. AVIRIS pixels are shortened in the cross track direction (20 x 15 m) because of the high altitude of the Venir site. Nearest neighbor resampling was avoided during the registration process because it was important to preserve all details of the mineral zones at this fine spatial scale. Pixel orientation is that of the original AVIRIS flight line direction.

the ellipse for each spectrum. Spectral averages for each station were corrected to absolute reflectance with a National Institute for Standards and Technology traceable spectralon standard, assembled into a traverse data cube, and then analyzed by Tetracorder to produce a traverse mineral map. Next, the AVIRIS mineral map was co-registered and overlain on a geographically registered color aerial photograph of the Venir pile (Figure 4).

The 26 surficial samples were analyzed for bulk chemical composition, leachate pH, leachate specific conductance, and metal leachability in USGS laboratories. Samples were dry sieved to < 4 mm and a portion digested and analyzed by inductively coupled plasma - atomic emission spectrometry. Another portion of the < 4 mm fraction of each sample was subjected to the Synthetic Precipitation Leach Procedure (*25*) that requires adding 2 liters of slightly acidified deionized water (initial pH = 4.2 using an H_2SO_4 / HNO_3 mixture) to 100 g of sample and agitating the mixture end-over-end at 30±2 rpm for 18 hours. Leachate pH and specific conductance were measured before filtering through a 0.7 μm Gelman Sciences TCLP glass fiber filter. Filtered leachates were acidified with concentrated HNO_3 and analyzed by inductively coupled plasma - mass spectrometry.

Mineralogic composition was determined for 11 surficial samples using XRD analysis. Samples were chosen from stations spread out along the traverse to provide a variety of samples from each spectral zone. XRD analyses were performed on mineral coatings/cements and bulk rock samples (Table 1). For

TABLE 1. Minerals Identified by XRD in the Venir Pile Traverse Samples

Traverse Station	Spectral Zone	Pyrite	Coquimbite	Jarosite	Goethite	Hematite	Amorph. Comp.	Kaolinite	Illite	Montmorillite	Muscovite	Clinochlore	Quartz	K-Feldspar	Plagioclase	Ankerite	Lanarkite
30m	G	–	–	tr	–	tr	tr	tr	–	–	m	tr	M	tr	tr	tr	tr?
50m	J+G	–	–	tr	–	–	M	tr	tr	–	–	–	M	tr	–	–	–
*80m	J+G	–/tr	–/–	m/tr	tr/tr	–/–	M/tr?	M/tr	tr/tr	–	–/m	–/–	M/M	M/m	m/–	–/–	–/–
100m	J	–	–	m	–	–	M	–	M	–	M	–	m	tr	tr	–	–
130m	J	m	–	tr	–	–	tr	tr	–	–	m	–	M	tr	–	–	–
*150m	J	m/tr	m/m	–/tr	–	–	m/–	tr/tr	–	–	m/tr	–/–	M/M	tr/tr	–	–	tr?
190m	G	–	–	m	m	–	tr	–	–	–	m	–	M	–	–	–	–
*200m	G	–/–	–/–	m/tr	tr/tr	–	M/tr	tr/tr	–	–	tr/tr	m/m	M/M	–/m	m/m	tr	–

Spectral Zones: J = Jarosite; J + G = Jarosite + Goethite; G = Goethite.
Components: M = Major; m = minor; tr = trace; tr? = possible trace.
* Has both surface and bulk XRD analyses. Amorph. Comp = amorphous component.
Surface = top 1 mm scraped from rock surface; Bulk = < 4 mm fraction.

Not Measured → (upper triangle) / Surface → tr (upper)
Not Detected → – (lower triangle) / Bulk → m (lower)

coatings, only the outer 1 mm of sample was scraped and analyzed by XRD. This sampling scheme comes closest to analyzing the surface mineralogy that imaging spectroscopy detects. As a check on how surface coatings differed from the mineralogy of the bulk sample, XRD analyses were performed on both the surface and < 4 mm fractions of a sample from each zone. All XRD analyses were run on a Philips APD 3720 automated diffractometer with powder mounts using Cu $K\alpha_1$ radiation.

Results and Discussion

Spectral Mineral Map. The AVIRIS mineral map of the Leadville area (Figure 2) shows that many of the pyritic waste piles are spectrally dominated by Fe-bearing secondary minerals. Topography plays a major role in shaping the zones because it controls the flow of surface runoff and hence the distribution of secondary minerals. In most cases, these secondary minerals occur in concentric zones that fan out downslope from the piles, but occasionally form nearly circular bull's-eye patterns as they do at the Venir waste rock pile (Figure 2). These zones usually consist of a central jarosite zone surrounded by a larger jarosite + goethite zone, that is itself surrounded by an even larger goethite zone. In places hematite dominates pixels within and at the edges of the goethite zones. Schwertmannite and ferrihydrite were not abundant enough to dominate spectrally over an entire pixel in this study area. It is possible that these

two secondary minerals are more abundant than is depicted on the mineral map, but their presence may be concealed beneath thin (~ 35 μm) optically opaque coatings of goethite (23). Alternatively, goethite may spectrally dominate these minerals in aerial and intimate mixtures as seen in laboratory measurements. In either case the presence of abundant goethite, the most stable of the hydrous Fe-oxides (6, 26), on a pile indicates that pyrite oxidation is at an advanced stage at the surface of the waste at that location.

Venir Pile Mineral Map. An enlargement of the AVIRIS mineral map centered on the Venir pile (Figure 4) shows a jarosite zone at the center of the mine-waste pile, surrounded by a discontinuous jarosite + goethite zone along the slopes and margins of the pile, in turn surrounded by a larger goethite zone at the base of the pile that is itself partially rimmed by a few isolated patches of hematite. Comparison of Figures 3 and 4 shows that spectral mineral zones cross color and albedo variations, which are mostly due to changes in grain size and not composition. This example indicates that color aerial photography cannot be used to reliably delineate the mineral zones.

The spectral traverse in Figure 4 shows that the goethite zone extends downslope to the west further into the forest than depicted on the AVIRIS mineral map. With the field spectrometer it was possible to selectively avoid vegetative cover and instead focus on bare areas between the vegetation, thus allowing the spectral traverse to be extended beyond the point where AVIRIS was unable to map surface mineralogy between the plants. Otherwise the correlation between the AVIRIS maps and the traverse mineral map is nearly one-to-one except near the man-made structures with rusted metal roofs and walls (Figure 3). These structures contribute a goethite spectral signature, which adds to that from nearby jarosite-coated mine waste, resulting in a combined jarosite + goethite spectral signature at the spatial scale of AVIRIS pixels. Ground spectra indicate that the actual jarosite zone extends between the buildings almost to the eastern margin of the pile. The geochemical measurements described below were keyed to mineral zones derived from the ground spectra, because of their finer spatial resolution.

Venir Pile Traverse Mineralogy. The correlation between bulk and surface mineralogy, as determined by XRD, is weak to moderate for the three samples representative of each spectral zone (Table 1). These changes probably reflect the destruction of phases

A

B
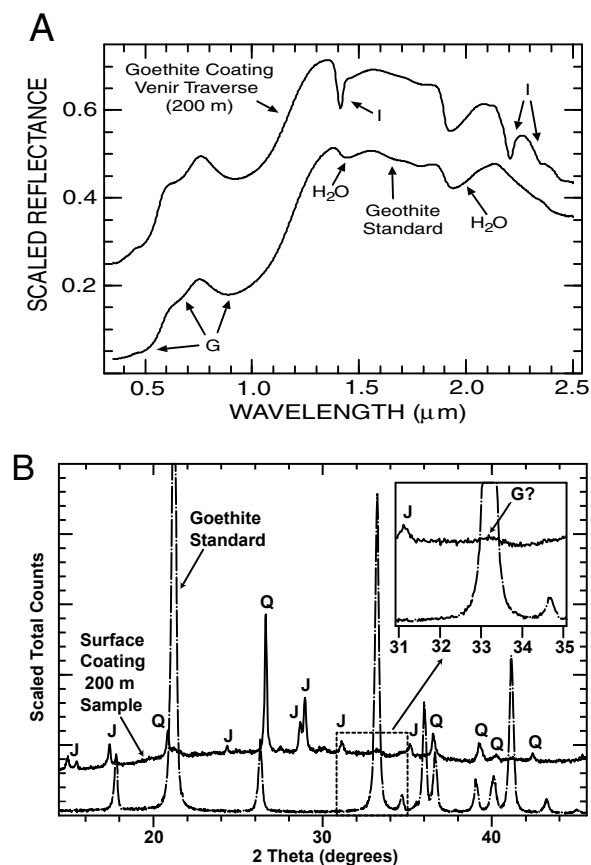
Figure 5. A) Reflectance spectrum of the goethite coating on a sample from the 200-m station along the Venir pile spectral traverse compared to a spectrum of a pure natural goethite standard. G = goethite absorption; I = illite absorption; H_2O = adsorbed water. Spectra offset vertically for clarity (main tick marks are 20% reflectance units apart). The goethite coating has absorptions that match the wavelength position and intensity of the goethite standard. B) XRD pattern of goethite coating scraped from the same 200 m station sample compared to the goethite standard. Patterns offset vertically for clarity (main tick marks are 1000 counts apart). Q = quartz peak; J = jarosite peak; G = goethite peak. Inset shows a very weak goethite reflection from the 200-m station sample compared to that of the goethite standard.

susceptible to weathering (e.g. pyrite and feldspars) and the formation of secondary minerals from oxidation of pyrite. Likewise, comparison of spectral zone mineralogy with that from XRD shows general agreement, with a few discrepancies. In particular,

only trace to minor amounts of goethite were detected on the surface of samples by the XRD procedure, which is consistent with earlier studies that indicate a relatively high spectral sensitivity to goethite compared to that of XRD (*23*). This discrepancy can be illustrated qualitatively with a sample from the Venir pile traverse. Figure 5A compares the reflectance spectrum of a goethite-coated rock collected from the 200-m station to that from a pure natural goethite standard. Spectral absorptions of the Venir sample strongly resemble those of the goethite standard when narrow absorptions at 1.43 and 2.2 μm from illite are ignored. This comparison confirms that the 200-m station sample contains spectrally abundant goethite. Figure 5B compares the XRD patterns of the same two samples. Most notable is the absence of well-defined goethite peaks from the 200-m station sample when compared to those of the goethite standard (inset Figure 5B).

The likely explanation is that the goethite coating the 200-m station sample is amorphous on the scale of XRD. Spectroscopic identification only requires order on the scale of molecular bonds whereas XRD requires longer range crystallographic order, making it difficult for XRD to identify poorly crystalline or nano-crystalline minerals. The presence of a broad rise in the XRD patterns of the surface samples (the so called "amorphous hump") indicates that the mine waste contains significant quantities of X-ray amorphous material (Table 1).

Venir Pile Traverse Geochemistry. Results of the leachate chemical analyses show excellent correlation between mine-waste pH, specific conductance, and spectral zone mineralogy. Figure 6 shows the leachate pH versus distance along the Venir traverse. Overall, pH varies from a low of 2.3 near the center of the pile to a high of 6.1 50 meters downslope from the western edge of the pile. Each spectral zone has its own distinct leachate pH range: 2.3 - 2.6 in the jarosite zone, 2.9 - 3.5 in the jarosite + goethite zone, and 4.5 - 6.1 in the goethite zone (Figure 6 and Table 2).

Leachable trace metal concentrations generally show a good correlation to the spectral mineral zones (Figure 7). The concentration versus distance profiles show that metal leachability in the goethite zone is a small fraction of that in the other spectral zones (except for Mn). In fact, leachate concentrations of Pb, Cu, As, and Co vary over three orders of magnitude across the spectral zones. It is evident from Figure 7 that bulk metal concentration is an unreliable predictor
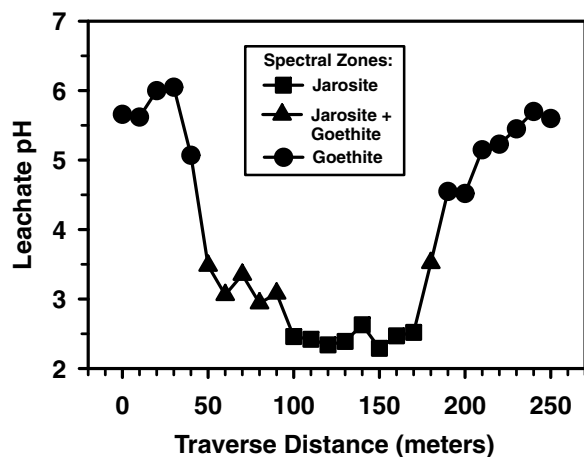
Figure 6. Synthetic Precipitation Leaching Procedure leachate pH versus distance along the Venir mine-waste pile traverse. Each spectral mineral zone is denoted by a different symbol.

of metal leachability. The increase in metal leachability in the jarosite and jarosite + goethite zones can be calculated by dividing the summed average leachable metal concentrations for each of these spectral zones by the summed average concentration for the goethite zone (from Table 2). Doing this gives a 10-fold increase in leachability for these trace metals in the jarosite + goethite zone and a 50-fold increase in the jarosite zone relative to the goethite zone. In general, jarosite and jarosite + goethite zones could pose a serious contamination threat if they are intersected by streams capable of transporting metal-rich water and suspended sediment.

Origin of the Secondary Mineral Zones. Analysis of the mineral maps and field observations suggest that in areas containing pyritic mine waste, there develops a chemical gradient from highly acidic, metal-rich water formed in close proximity to the waste, to more neutral less metal-rich water away from the waste piles. As pyrite oxidation progresses, this gradient causes the sequential deposition of different secondary minerals under progressively less acidic conditions in roughly concentric zones on and around the piles. Because pH is an important control on the stability of the Fe-bearing secondary minerals (6), the mineralogic identities of the secondary minerals may record the pH conditions of their formation. The secondary mineral zones also provide estimates of metal leachability, because trace metal leachability is controlled to an extent by pH (27).

Jarosite has an important role in the formation of

the secondary mineral zones because it can become unstable when exposed to water from snowmelt or rainfall. Baron and Palmer (28) have studied the solubility of synthetic K-jarosite and suggest that it transforms to ferric oxyhydroxide when pH increases. They give a transformation reaction

$$KFe_3(SO_4)_2(OH)_6 + 3H_2O \rightleftharpoons$$
$$3Fe(OH)_{3(s)} + K^+ + 2SO_4^{2-} + 3H^+ \quad (1)$$
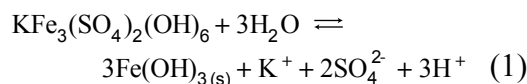
which generates acidity. According to their work, the pH stability field for jarosite is a function of the solubility products of jarosite and $Fe(OH)_{3(s)}$, and the activities of K^+ and SO_4^{2-}. Using their solubility product numbers and averaged annual chemical analyses of precipitation for the last five years collected by three weather stations within a 100 km radius of Leadville (29), we calculate that jarosite in contact with snowmelt or rainfall with $[K^+] = 6.6 \times 10^{-7}$ mol/L and $[SO_4^{2-}] = 6.4 \times 10^{-6}$ mol/L has a transition pH of 3 (using concentrations instead of activities for K^+ and SO_4^{2-}). Low-temperature jarosites, often found in mine waste, may contain H_3O^+ replacing K^+ or excess H_2O charge-balancing Fe^{3+} deficiencies (28). The presence of H_3O^+ or excess H_2O in jarosite also lowers the pH of this transformation. Although thermodynamics favor jarosite transformation in the presence of precipitation, questions remain about the rate of the transformation. It seems probable that weathering will initially transform jarosite exposed at the surface of the waste, and this is precisely where spectral measurements are taken. $Fe(OH)_{3(s)}$ or its probable mineralogic equivalent, ferrihydrite, is unstable and eventually transforms to goethite or hematite (30).

In a theoretical sense, the secondary mineral zones represent evolving stages of the oxidation process. Initially, oxidation of pyritic waste at the surface produces a jarosite zone rich in efflorescent salts such as melanterite [$Fe^{II}SO_4 \cdot 7H_2O$] and copiapite at the center of the pile. The presence of these salts and pyrite stabilize jarosite because of their high capacity to directly and indirectly generate acidity and dissolved SO_4^{2-}. As weathering proceeds, a jarosite + goethite zone forms on the slopes of the waste pile where erosion of fine-grained waste leaves a lag deposit of coarser pyrite-rich rock. Erosion in this zone continually exposes fresh pyrite that oxidizes producing jarosite. Subsequent exposure to precipitation causes the jarosite to transform to
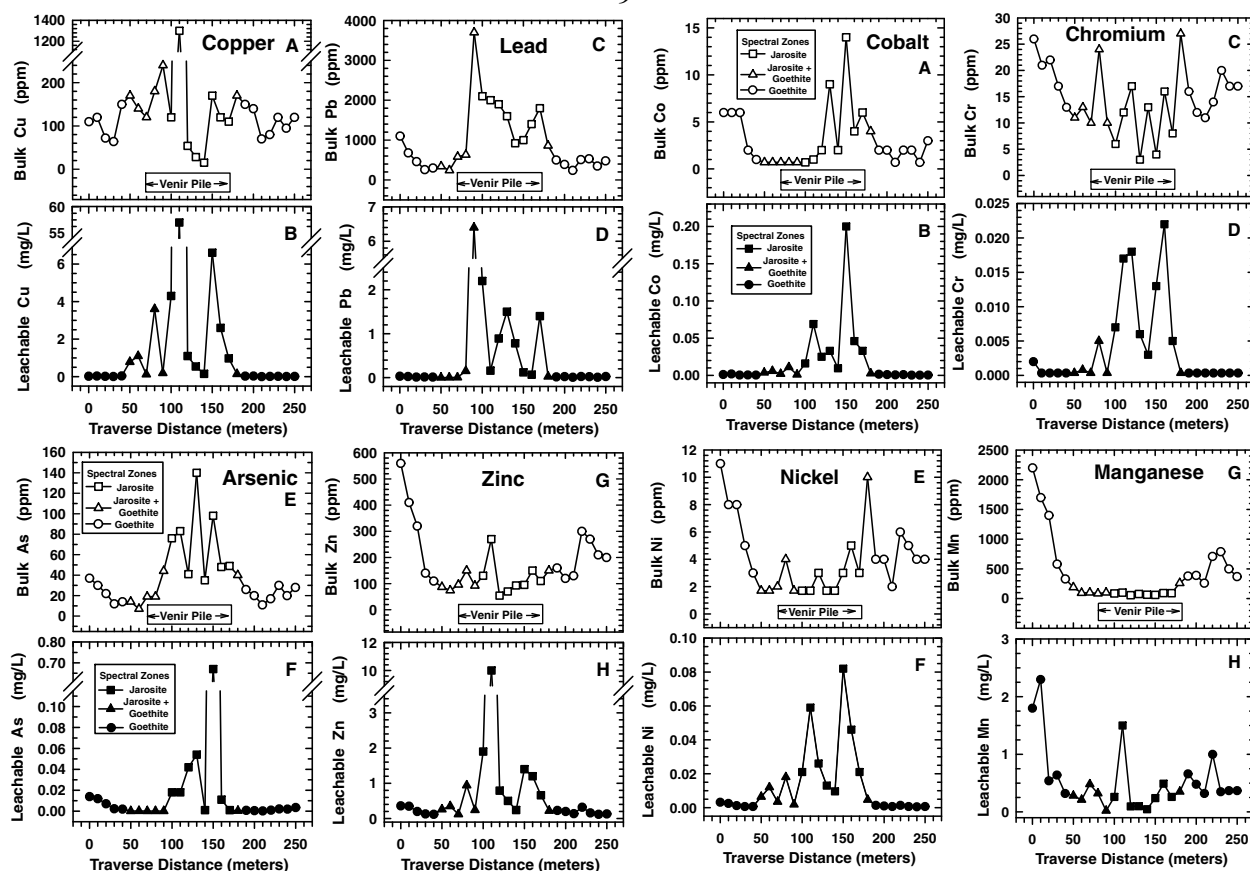
Figure 7. A) Bulk (< 4 mm fraction) and Synthetic Precipitation Leaching Procedure leachate concentrations of Cu, Pb, As, and Zn versus distance along the Venir mine-waste pile traverse. B) Bulk and leachate concentrations of Co, Cr, Ni, and Mn versus distance along the Venir mine-waste pile traverse. Each spectral mineral zone is denoted by a different symbol.

Table 2. Range of Geochemical Values for the Venir Mine-Waste Pile Spectral Mineral Zones

geochemical parameter	jarosite zone (8 samples)		jarosite+goethite zone (6 samples)		goethite zone (12 samples)	
	avg.	range	av	range	av	range
pH	2.4	2.3-2.6	3.2	2.9-3.5	5.4	4.5-6.1
specific conductance(μS/cm)	2110	1170-3870	317	158-675	41	20-100
bulk metals[a] (ppm) ΣZn+Cu+Cd+Pb+Co+Ni	1690	1030-3570	1340	450-4030	850	440-1800
leachable metals[b](mg/L) ΣZn+Cu+Cd+Pb+Co+Ni	12.25	1.19-67.5	2.46	0.25-6.83	0.25	0.14-0.42

[a]Bulk metals from < 4 mm sample fraction. [b]Leachable metals from the Synthetic Precipitation Leaching Procedure performed on the < 4 mm sample fraction.

ferrihydrite which eventually transforms to goethite or hematite. Meanwhile, a goethite zone forms at the toe of the pile where acidic metal-rich water leaves the pile and is diluted by precipitation or buffered by reacting with surrounding rock. As the oxidation of pyrite progresses in the pile, the goethite zone expands at the expense of the jarosite zone, theoretically at least until all the pyrite at the surface is exhausted, and the last remnants of the jarosite zone transform to goethite. The AVIRIS mineral map (Figure 4) and field

observations show that goethite appears to be the dominant product of jarosite decomposition at the Venir pile.

Guidelines for Using the Screening Tool. As demonstrated at the Venir pile, areas with jarosite at the surface have an elevated potential for generating acidic water. However, questions remain about the reliably of using jarosite as a universal indicator of acid-generating potential. For instance, if jarosite is stabilized to near-neutral pH by high concentrations of K^+ and SO_4^{2-}, or if remnant jarosite persists outside of its pH stability range because of slow reaction kinetics, then its associated minerals need not be capable of generating acid. Yet, jarosites exposed at the surface are the most vulnerable to transformation, because K^+ and SO_4^{2-} are usually removed from the surface first by weathering and subsequent leaching. Thus, the persistence of jarosite at the surface is more likely to reflect ongoing oxidation of pyrite rather than past acidic conditions. Clearly, additional pH and metal leachability tests need to be conducted on wastes from different deposit types weathering under different climatic conditions to settle this possible ambiguity. Pending the results of these additional tests, it may not be prudent to interpret the presence of jarosite as unconditional proof of high acid-generating capacity. Nevertheless, the presence of jarosite does indicate that these areas need closer examination.

This screening tool is best suited for locating acidic minerals exposed at the surface and evaluating the potential for acidic drainage at the surface. Exactly how well surface mineralogy predicts subsurface acidity and metal leachability needs further study. Areas lacking jarosite at the surface may still generate acidic drainage. Another, sometimes substantial, source of acidic metal-rich water is that which flows out of seeps or drainage tunnels, usually called acid mine drainage (*27*). These sources may not be obvious on mineral maps because of their small size relative to the large footprint of an AVIRIS pixel, though finer spatial resolution data may help overcome this difficulty. Perhaps the most potent source of metals is from easily dissolved efflorescent salt crusts (*7, 27*). These metal-rich salts can form in and outside of jarosite zones, providing a nearly-instantaneous source of acid and metals. Fortunately, most of these crusts can also be spectrally mapped by detecting intense H_2O absorptions caused by fluid inclusions in the salt (*31*).

The screening tool may not be suitable for evaluating remediated mine waste because the original distribution of secondary mineral zones may be disturbed or concealed beneath a cap of neutral material and vegetation. However, vegetation alone may not pose much of a detection problem at the worst sites, because the high acidity and metals associated with pyritic mine waste tend to prevent the growth of vegetation, leaving the waste exposed and suitable for detection with remote sensing. Consequently, this screening tool can be used not only in arid regions but also in densely vegetated areas where acid and metal concentrations are high enough to defoliate the surface.

The EPA estimates (*32*) that mineral maps made from AVIRIS data at Leadville accelerated remediation efforts by two years saving over $2 million in investigation costs. It took about two months to compile mineral maps highlighting mine waste mineralogy with the highest potential to generate acidic drainage. The U.S. Bureau of Reclamation and the EPA used these maps to prioritize field sampling of mine-waste sites, thus reducing sampling and interpretation time by more than two years.

Acknowledgments

Literature Cited

(1) Ferderer, D.A. *U.S. Geological Survey Open-File Report 95-549,* **1996,** 42 p.
(2) Green, R.O; Eastwood, M.L; Sarture, C.M.; Chrien, T.G.; Aronsson, M.; Chippendale, B.J.; Faust, J.A.; Pavri, B.E.; Chovit, C.J.;

Solis, J.; Olah, M.R.; Williams, O. *Remote Sens. Environ.* **1998**, 65, 227-248.

(3) Clark, R.N.; Gallagher, A.J.; Swayze, G.A. *Jet Propulsion Laboratory Pub. 90-54,* **1990**, 176-186.

(4) Boardman, J.W.; Huntington, J.F. *Jet Propulsion Laboratory Pub. 96-4, 1,* **1996**, 9-11.

(5) Nordstrom, D.K. In *Acid Sulfate Weathering;* Kittrick, J.S., Fanning, D.S., Hossner, L.R., Kral, D.M., Hawkins, S., Eds.; Soil Society of America: 1982, p. 37-56.

(6) Bigham, J.M.; Schwertmann, U.; Carlson, L. In *Biomineralization: Processes of Iron and Manganese,* Skinner, H.C.W.; Fitzpatrick, R.W., Eds.; Catena Supplement 21: Cremlingen-Destedt, Germany: **1992**, 219-232.

(7) Alpers, C.N.; Blowes, D.W.; Nordstrom, D.K.; Jambor, J.L. In *The Environmental Geochemistry of Sulfide Mine-Wastes, Short Course Handbook;* vol. 22; Jambor, J.L.; D.W. Blowes, Eds.; Mineralogic Association of Canada: Waterloo, Ontario, Canada: **1994**; 247-270.

(8) Bigham, J.M.; Schwertmann, U.; Traina, S.J.; Winland, R.L.; Wolf, M. *Geochimica et Cosmochimica Acta* **1996**, *60,* 2111-2121.

(9) Bigham, J.M. In *The Environmental Geochemistry of Sulfide Mine-Wastes, Short Course Handbook;* vol. 22; Jambor, J.L.; D.W. Blowes, Eds.; Mineralogic Association of Canada: Waterloo, Ontario, Canada: **1994**; 103-132.

(10) Fleischer, M.; Mandarino, J.A. *Glossary of Mineral Species;* The Mineralogical Record Inc.: Tucson, Arizona: **1995**, 280p.

(11) Swayze, G.A.; Clark, R.N.; Pearson, R.M.; Livo, K.E. *Jet Propulsion Laboratory Pub. 96-4, 1,* **1996**, 231-234.

(12) Swayze, G.A.; Clark, R.N.; Smith, K.S.; Hageman, P.L.; Sutley, S.J.; Pearson, R.M.; Rust, G.S.; Briggs, P.H.; Meier, A.L.; Singleton, M.J.; Roth, S. *Jet Propulsion Laboratory Pub. 97-21, 1,* **1998**, 385-389.

(13) Kruse, F.A.; Hauff, P.L.; Dietz, J.; Brock, J.C.; Hampton, L. Final Report Contract #412.DEN.63786.FM (CH2M HILL), Center for the Study of Earth from Space, Univ. of Colorado, Boulder, **1989**, 79 p.

(14) King, T.V.V.; Clark, R.N., Ager, C.; Swayze, G.A. *Proceedings: Summitville Forum '95*:

Posey, H.H.; Pendelton, J.A.; Van Zyl, D., Eds.; Colorado Geological Survey Special Publication 38: **1995**, 59-63.

(15) Farrand, W.H.; Harsanyi, J.C. *Remote Sensing of Environment* **1997**, *59*, 64-76.

(16) Fenstermaker, L.K.; Miller, J.R. *Photogrammetric Engineering and Remote Sensing* **1994**, *60,* 989-995.

(17) Emmons, S.F.; Irving, J.D.; Loughlin, G.F. *U.S. Geological Survey Prof. Pap. 148,* **1927**, 368p.

(18) Pearson, R.M. *Environmental Geology of Operable Unit 6 Removal Action Design Data California Gulch Superfund Site Leadville, Colorado*: U.S. Bureau of Reclamation Technical Document, **1997**, 42 p.

(19) Clark, R.N.; Swayze, G.A.; Gallagher, A.J.; King, T.V.V.; Calvin, W.M. *U.S. Geological Survey Open File Report 93-592,* **1993**, 1326 p.

(20) Gao, B.C; Heidebrecht, K.B.; Goetz, A.F.H. *Remote Sensing of Environment* **1993**, *44*, 165-178.

(21) Clark, R.N.; Swayze, G.A.; Heidebrecht, K.; Green, R.O.; Goetz, A.F.H. *Jet Propulsion Laboratory Publication 95-1,* **1995**, 41-42.

(22) Clark, R.N.; Swayze, G.A. *Jet Propulsion Laboratory Publication 95-1,* **1995**, 39-40.

(23) Buckingham, W.F.; Sommer, S.E. *Economic Geology* **1983**, *78*, 664-674.

(24) Swayze, G.A. *The hydrothermal and structural history of the Cuprite Mining District, southwestern Nevada: an integrated geological and geophysical approach,* Ph. D. Dissertation, University of Colorado at Boulder, **1997**, 399 p.

(25) U.S. Environmental Protection Agency *Test Methods for Evaluating Solid Waste, Physical /Chemical Methods (SW-846)*, 3rd Edition, update 3B, National Center for Environmental Publications, Cincinnati, OH 45268, phone 800-553-6847, order no. EPASW-846.3.2B. Accessed (8/1/99) at URL <http://www.epa.gov/epaoswer/hazwaste/test/sw846.htm>.

(26) Alpers, C.N.; Brimhall, G.H. *Economic Geology* **1989**, *84,* 229-255.

(27) Plumlee, G.S.; Smith K.S.; Montour, M.R.; Ficklin, W.H.; Mosier, E.L. In *Reviews in Economic Geology, Part B: Case Studies and*

Research Topics L.H. Filipek; Plumlee, G.S., Eds.; Society of Economic Geologists, **1999,** 373-432.

(28) Baron, D.; Palmer, C.D. *Geochimica et Cosmochimica Acta,* **1996**, *60*, 185-195.

(29) National Atmospheric Deposition Program (NRSP-3)/National Trends Network (1999), NADP Program Office, Illinois State Water Survey, 2204 Griffith Drive, Champaign, IL 61820.

(30) Jambor, J.L.; Dutrizac, J.E. *Chemical Review* **1998**, *98*, 2549-2585.

(31) Pearson, R.M.; Swayze, G.A.; Wiltshire, R.; Serina, D.; Clark, R.N. *Proceedings of the 3rd International Airborne Remote Sensing Conference* Copenhagen, Denmark, July, **1997**, I-102 - I-109.

(32) U.S. Environmental Protection Agency *Advanced Measurement Initiative Workshop Report EPA-235-R-98-002,* 1998, 22 p.

Supplementary Materials Section Follows On Next Page

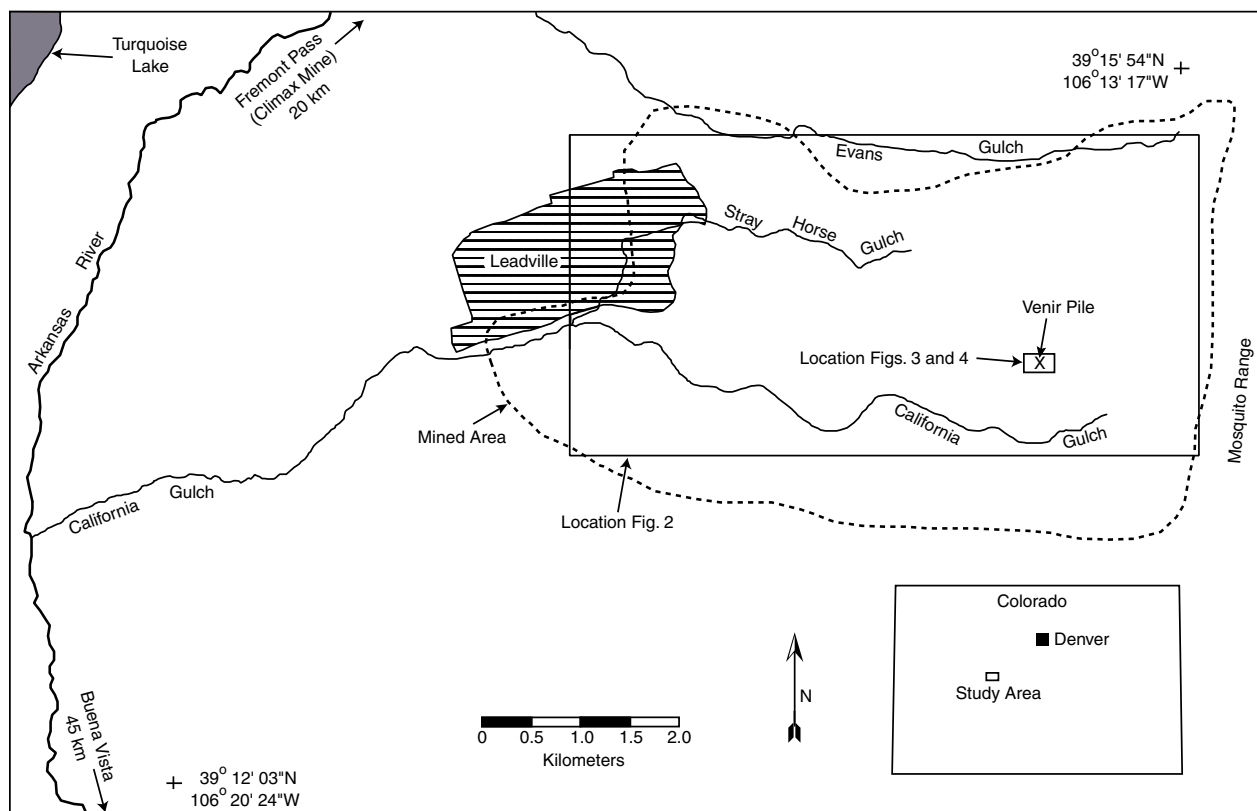For more information on imaging spectroscopy see the USGS Denver Spectroscopy website: http://speclab.cr.usgs.gov

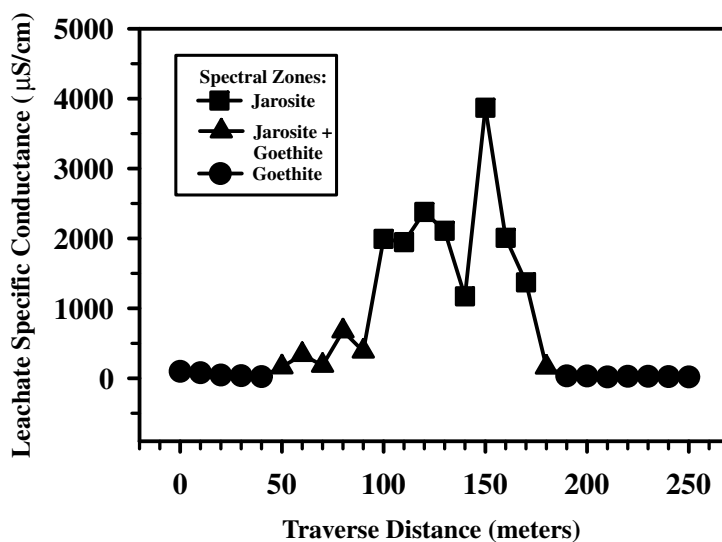**Figure S1. Location of study site showing areas of figures 2, 3, and 4.**

Figure S2. Synthetic Precipitation Leaching Procedure leachate specific conductance versus distance along the Venir mine-waste pile traverse. Jarosite zone leachates have higher specific conductance values than do leachates from the other spectral mineral zones. Specific conductance closely follows the SO_4^{2-} concentrations in the leachates, varying from a high of 3870 μS/cm near the center of the pile to a low of 20 μS/cm at the eastern end of the traverse. Similar to pH, each spectral zone has its own distinct range of leachate specific conductance (μS/cm): 3870 - 1170 in the jarosite zone, 675 - 158 in the jarosite + goethite zone, 100 - 20 in the goethite zone.
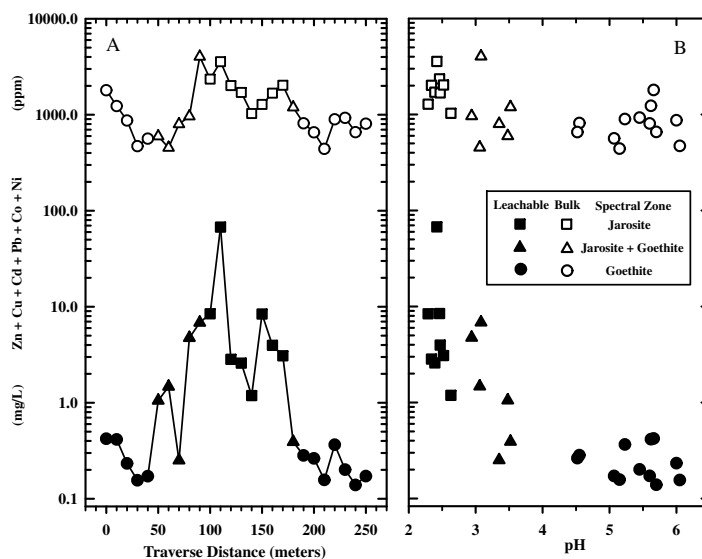
Figure S3. A)Concentrations of the sum of selected bulk (< 4 mm fraction) and leachable trace metals along the Venir mine-waste pile traverse. B) Ficklin plot of the sum of leachate trace metals versus leachate pH.
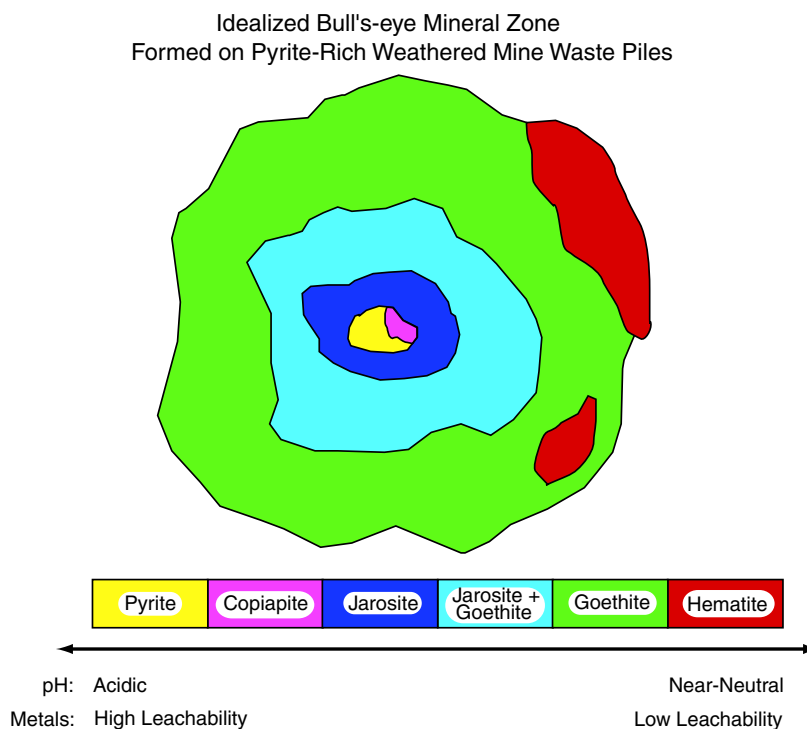
Idealized Bull's-eye Mineral Zone
Formed on Pyrite-Rich Weathered Mine Waste Piles

Figure S4. Idealized bull's-eye pattern of spectrally detectable Fe-bearing secondary mineral zones. Leachate pH is low and metal leachablity high in the central pyrite, copiapite, and jarosite spectral mineral zones, while leachate pH is high and metal leachability low in the outer goethite and hematite zones. The jarosite + goethite zone has average leachate pH and metal leachability values between those of the surrounding zones. This model has been developed from this study and observations at other mine sites. An idealized sequence from high to low acidity and metal leachability is pyrite=copiapite > jarosite > goethite ≥ hematite. In the model, the pyrite zone may be partially or totally obscured by a coating of jarosite ± copiapite, and the goethite zone maybe partially surrounded by a discontinuous hematite zone.